Electronic Supplementary Material (ESI) for Physical Chemistry Chemical Physics.
This journal is © the Owner Societies 2023

ReaxFF Molecular Dynamics of Graphene Oxide/NaCl Aqueous Solution Interfaces

Rokhsareh Akbarzadeh[a], Milan Předota*[b]

Received 00th January 20xx,
Accepted 00th January 20xx

DOI: 10.1039/x0xx00000x

Supplementary information

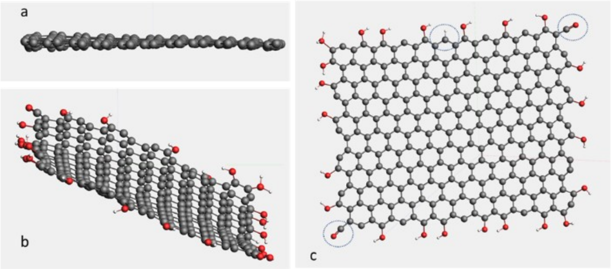

Figure S1 a) Side view of initial graphene, b) & c) side view and top view of graphene after interaction with saline water for 1ns (hydroxyl and carbonyl groups formed at the edge of graphene, carbonyl groups highlighted by circles).

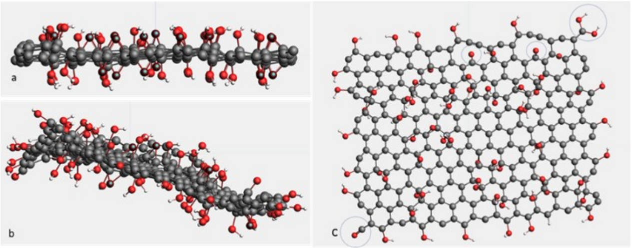

Figure S2 a) Side view of initial GO structure before interaction with water and b) & c) the top view and the side view of single layer GO after interaction with saline water for 1ns (carbonyl and diol groups formed on the sheet have been highlighted by larger circles.

Table S1 Total surface charge of a graphene or graphene oxide sheet including functional groups at different times indicating its stabilization and evolution due to surface reactions.

Total Surface Charge (e)	0 ns	1 ns	2 ns	3 ns
Graphene	-4.165	-4.294	-6.580	-7.005
Graphene oxide	-2.700	-11.705	-11.377	–

Table S2 Average relative abundances of species in the systems.

Molecules	G	GO	GTO
	Number	Number	Number
H_2O	1900	1850	2683
Cl	30	28	44
Na	30	28	42
NaOH	0	12	18
H_3O	25	6	11
OH	-	10	34
Na_2OH	-	7	9
Na_2	10	5	7
$Na(OH)_2$	-	4	8
$Na_2(OH)_2$	-	3	5
HCl	3		-
O_2	-	-	2

Table S3 Analysis of reaction events in the systems during the 1 ns production run. Only reactions with the number of events >30 are listed.

No	G			GO			GTO		
1	Reaction	Rate constant	Number of events	Reaction	Rate constant	Number of events	Reaction	Rate constant	Number of events
2	$H+H_2O \rightarrow H_3O$	6.109×10^{12}	2820	$Na+ OH \rightarrow HNaO$	8.336×10^{13}	482	$H+H_2O \rightarrow H_3O$	7.798×10^{12}	789
3	$H_3O \rightarrow H+H_2O$	9.439×10^{10}	2592	$HNaO \rightarrow Na+ OH$	8.966×10^{10}	475	$H_3O \rightarrow H+H_2O$	1.474×10^{11}	743
4	$H_3O+H_2O \rightarrow H+H_2O+H_2O$	5.218×10^{11}	445	$H+H_2O \rightarrow H_3O$	8.205×10^{12}	443	$Na+ OH \rightarrow HNaO$	1.103×10^{14}	591
5	$H+OH \rightarrow H_2O$	1.152×10^{16}	369	$H_3O \rightarrow H+H_2O$	1.182×10^{11}	415	$HNaO \rightarrow Na+ OH$	5.380×10^{10}	568
6	$H2O \rightarrow H+ OH$	1.684×10^{8}	337	$H+ OH \rightarrow H_2O$	5.463×10^{14}	152	$H+ OH \rightarrow H_2O$	9.324×10^{14}	458
7	$H+H_2O+H_2O \rightarrow H_3O+H_2O$	1.250×10^{13}	205	$H_2O \rightarrow H+ OH$	6.289×10^{7}	146	$H_2O \rightarrow H+ OH$	1.235×10^{8}	427
8	$H_3O+H_2O+H_2O \rightarrow H+H_2O+H_2O+H_2O$	1.090×10^{12}	42	$H_3O+H_2O \rightarrow H+H_2O+H_2O$	4.847×10^{11}	74	$H_3O+H_2O \rightarrow H+H_2O+H_2O$	7.211×10^{11}	124
9	$H_2O+H_2O \rightarrow H_3O+ OH$	3.567×10^{8}	32	$OH +HNaO \rightarrow H_2NaO_2$	6.881×10^{13}	60	$OH +HNaO \rightarrow H_2NaO_2$	7.237×10^{13}	99
10	$H+H_2O+H_2O+H_2O +H_2O \rightarrow H_3O+H_2O+H_2O$	4.246×10^{13}	29	$H_2NaO_2 \rightarrow OH +HNaO$	1.06×10^{11}	54	$H_2NaO_2 \rightarrow OH +HNaO$	2.786×10^{10}	76
11	$C_{264}H_{23}O_{24}+ OH \rightarrow C_{264}H_{24}O_{25}$	1.630×10^{13}	34	$H+H_2O+H_2O \rightarrow H_3O+H_2O$	1.630×10^{13}	39	$H+H_2O+H_2O \rightarrow H_3O+H_2O$	1.909×10^{13}	68
12				$C_{264}H_{22}O_{24}+ OH \rightarrow C_{264}H_{23}O_{25}$	8.480×10^{16}	59	$OH +H_2NaO_2 \rightarrow H_3NaO_3$	1.049×10^{14}	39
13							$H_3NaO_3 \rightarrow OH +H_2NaO_2$	4.285×10^{10}	31
14							$C_{264}H_{62}O_{74}+ OH \rightarrow C_{264}H_{63}O_{75}$	5.726×10^{13}	1
15							$C_{264}H_{62}O73+ H \rightarrow C_{264}H_{63}O_{73}$	2.987×10^{11}	11

---

[a] Department of Physics, Faculty of Science, University of South Bohemia, Branišovská 1760, 370 05 České Budějovice, Czech Republic

[b] Department of Physics, Faculty of Science, University of South Bohemia, Branišovská 1760, 370 05 České Budějovice, Czech Republic, predota@prf.jcu.cz

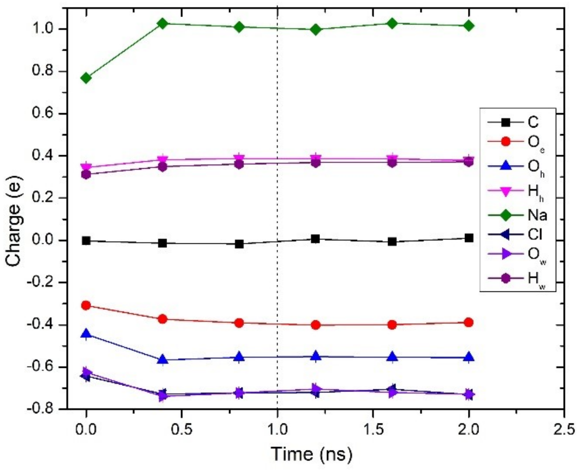

Figure S3 Average charges of atoms of each type as a function of time, showing only small oscillations around equilibrated values after the initial changes below 0.4 ns. The vertical dotted line at 1 ns indicates the beginning of the production run.

Figure S4 compares the RDFs of 0.8 M NaCl aqueous solution (30 NaCl pairs and 2100 water molecules) at 300 K and 1 bar obtained using 5 different parameterisations. These include the Joung and Cheatham NaCl forcefield[1], Chandrasekar[2] forcefield implemented in OPLS (atomic types opls_405 for Na$^+$ and opls_401 for Cl$^-$), the currently default newer OPLS model of Na$^+$ by Åqvist[3] (atomic types opls_407 for Na$^+$ 401 and keeping Cl$^-$ opls_401, and the Madrid-2019 forcefield[4] with ionic charges scaled to ±0.85 e. Except Madrid-2019, the forcefields apply Lorentz-Berthelot combining rule. The water models used in combination with these ionic models are listed in Table S4 together with the ionic parameters. In ReaxFF the water molecules are not explicitly defined as individual entities, but rather their interactions are captured through the reactive potential energy terms that govern bond breaking and formation. However, the developers of the used ReaxFF forcefield in this study[5], in one of their references[6] they mentioned that they modeled the water using the rigid, nondissociative, and nonpolarizable SPC/E model by Berendsen[7] and the dissolved ions as charged Lennard–Jones spheres.

Table S4 Parameters of ions used to compare their structure in 0.8 M NaCl solution.

Ion	*q* [e]	σ [Å]	ε [kJ/mol]	Water model	Reference
Na$^+$ JC	+1	2.15954	1.47545	SPC/E[7]	[1]
Cl$^-$ JC	-1	4.83045	0.05349	SPC/E[7]	[1]
Na$^+$ OPLS	+1	3.33045	0.011598	SPC[9]	[3]
Cl$^-$ OPLS	-1	4.41724	0.492833	SPC[9]	[2]
Na$^+$ OPLS_405	+1	1.89744	6.72427	SPC[9]	[2]
Na$^+$ Madrid	+0.85	2.21737	1.472356	TIP4P/2005[10]	[4]
Cl$^-$ Madrid	-0.85	4.69906	0.076923	TIP4P/2005[10]	[4]
Na$^+$	variable	2.983	0.03	SPC/E[7]	[5]
Cl$^-$	variable	3.947	0.227	SPC/E[7]	[5]

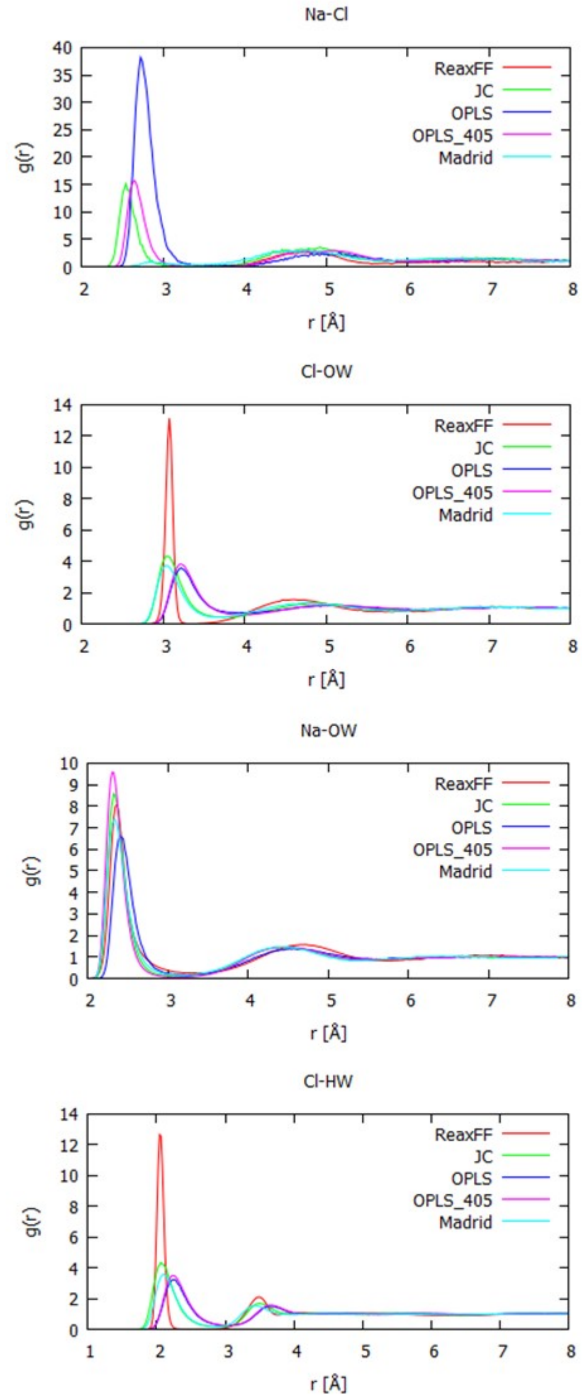

Figure S4 Comparison of radial distribution functions obtained with ReaxFF, Joung and Cheatham ions with SPC/E water (JC), current OPLS potentials for ions with (OPLS), the older model of Na$^+$ by Chandrasekar (OPLS_405), and Madrid 2019 force field with charges of ions scaled to 85% of their nominal values (Madrid).

The Na-Cl RDF exhibits strong contact peaks below 3 Å for the JC and OPLS force fields with full ionic charges, particularly for the currently default Na$^+$ parameterization (opls_407). Note that the older Na$^+$ parameterization[2] is quite close to the popular Joung and Cheatham's force field (FF)[1]. These strong peaks however were found[8] to cause overstructuring of the aqueous solutions, low solubilities and poor agreement with ab initio calculations and scattering experiments. Instead, Madrid-2019 forcefield features only small contact peak at 2.9 Å, while ReaxFF has no contact peak at all. The position of the second peak at 4.6-5.2 Å is predicted by all FFs similarly.

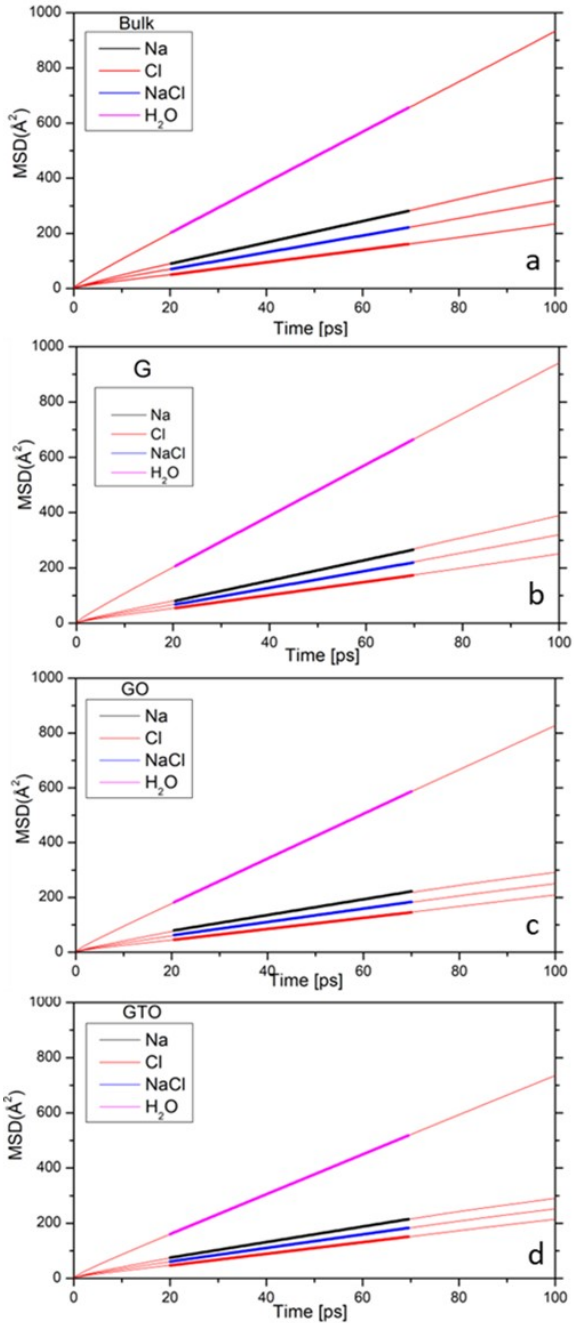

Figure S5 The mean square displacement for Bulk (a), G(b), GO (c) and GTO (d) systems. The fitted regions are highlighted.

The Na-Ow RDFs show that all FFs perform nearly identically, which indicates that the Na$^+$ model of ReaxFF is correct. However, the Cl-Ow and Cl-Hw RDFs reveal that the Cl$^-$ model of ReaxFF is overstructured, resulting in extremely high and narrow contact peak at 3.1 Å (Cl-Ow), resp. 2.1 Å (Cl-Hw). The overstructuring is also manifested by a steep drop of the first peak and extremely low minimum between the contact and solvent separated pairs, with the minimum of Cl-Ow being lower than 0.01. All these facts indicate very strongly bound 1st hydration shell of water around Cl$^-$, which definitely contributes to too low diffusivity of Cl$^-$. At the same time, the positions of the Cl-Ow and Cl-Hw peaks agree well for all forcefields. This stresses the necessity of investigating the dynamic properties of models and their inclusion into model parametrizations, as without that structurally correct but dynamically inaccurate models can result.

References

1 I. S. Joung and T. E. Cheatham, Determination of alkali and halide monovalent ion parameters for use in explicitly solvated biomolecular simulations, *Journal of Physical Chemistry B*, 2008, **112**, 9020–9041.

2 J. Chandrasekhar, D. C. Spellmeyer and W. L. Jorgensen, Energy component analysis for dilute aqueous solutions of Li$^+$, Na$^+$, F$^-$, and Cl$^-$ ions, *J. Am. Chem. Soc.*, **1984**, 106, 903-910.

3 J. Åqvist , Ion-Water Interaction Potentials Derived from Free Energy Perturbation Simulations, *J. Phys. Chem.*, 1990, **94**, 8021-8024.

4 I. M. Zeron, J. L. F. Abascal and C. Vega, A force field of Li$^+$, Na$^+$, K$^+$, Mg^{2+}, Ca^{2+}, Cl$^-$, and SO4^{2-} in aqueous solution based on the TIP4P/2005 water model and scaled charges for the ions, *Journal of Chemical Physics*, 2019, **151**, 134504.

5 S. Y. Kim, A. C. T. Van Duin and J. D. Kubicki, Molecular dynamics simulations of the interactions between TiO$_2$ nanoparticles and water with Na$^+$ and Cl$^-$, methanol, and formic acid using a reactive force field, *J Mater Res*, 2013, **28**, 513–520.

6 S. Y. Kim, N. Kumar, P. Persson, J. Sofo, A. C. T. Van Duin and J. D. Kubicki, Development of a ReaxFF reactive force field for titanium dioxide/water systems, *Langmuir*, 2013, **29**, 7838–7846.

7 H. J. C. Berendsen, J. R. Grigera and T. P. Straatsma, The Missing Term in Effective Pair Potentials, 1987, *J. Phys. Chem.*, **91**, 6269–6271.

8 M. Kohagen, P. E. Mason and P. Jungwirth, Accounting for Electronic Polarization Effects in Aqueous Sodium Chloride via Molecular Dynamics Aided by Neutron Scattering, *J. Chem. Phys. B*, 2016, **120**, 1454-1460.

9 H. J. C. Berendsen, J. P. M. Postma, W. F. Van Gunsteren and J. Hermans, *Intermolecular Forces*, 1981. Pullmann, B., Ed.; Reidel Press: Dordrecht, 331-334.

10 J. L. F. Abascal, E. Sanz, R. G. Fernández and C. Vega, A general purpose model for the condensed phases of water: TIP4P/2005, *J. Chem. Phys.,* 2005, **123**, 234505.